Iranian Journal of Oil & Gas Science and Technology, Vol. 10 (2021), No. 4, pp. 85-99
http://ijogst.put.ac.ir

Modeling of Gel-acid Injection for Optimizing the Acidizing Process and Comparing It with Core Injection Experimental Data: Case Study in One of Iranian Southwest Oilfields

Abdorrahman Mehri Ghahfarrokhi [1], Hassan Shokrollahzadeh Behbahani[2*], Ezzatollah Kazemzadeh[3] and Gholam Abbas Safian[4]

[1] M.S. Student, Reservoir Studies Department, Iranian Offshore Oil Company, Tehran, Iran.
[2] Assistant Professor, Department of Petroleum Engineering, Petroleum University of Technology, Ahwaz, Iran
[3] Assistant Professor, Research Institute of Petroleum Industries, Tehran, Iran.
[4] M.S. Student, National Iranian South Oil Company, Ahwaz, Iran

Highlights

- Two different VESs is injected in core plugs.
- Parallel acid core flood set-up is used.
- Viscosity measurement tests are run.

Received: September 29, 2021; *revised:* November 17, 2021; *accepted:* December 11, 2021

Abstract

Nowadays, use of visco-elastic surfactants as the main component of gel diverters is becoming more and more common among well completion engineers, as well as stimulation service companies. Gel diverter, as other kinds of diverters, is used in multi-layered carbonated reservoirs to diver acid into less permeable sublayer. As use of these materials becomes more common, modeling and simulating the gel-acid injection process becomes more required. In this study, a mathematical model is generated to simulate gel-acid injection process, and experimental data is compared with data predicted by the model. The purpose of this study is to investigate the field possibility of injection gel-acid and to generate a model for simulating this process, in order to smart permeability enhancement in Ahwaz oilfield, one of Iranian Southwest oilfields. The solutions predicted by model are in an acceptable correlation with experimental data. The generated model can be used for other multi-layered carbonated oilfields.

Keywords: Acidizing, Modeling, Multi-layered reservoirs, Stimulation, VES.

How to cite this article
Mehri Ghahfarrokhi. A, Shokrollahzadeh Behbahani. H, Kazemzadeh. E, Safian. Gh.A, Modeling of Gel-acid Injection for Optimizing the Acidizing Process and Comparing It with Core Injection Experimental Data: Case Study in One of Iranian Southwest Oilfields , Iran J. Oil Gas Sci. Technol., Vol. 10, No. 4, p.85-99, 2021.
DOI: http://dx.doi.org/10.22050/ijogst.2022.213717.1531, *This is an Open Access article under Creative Commons Attribution 4.0 International License. (creativecommons.org/licenses/by/4.0)/*

* Corresponding author :
Email: shokrollahzadeh@put.ac.ir

1. Introduction

There are three fundamental techniques used in acidizing treatments: wellbore clean-up (fill-up and soak of acid in the wellbore for cleaning it and string), matrix acidizing (injecting acid into the matrix pore structure with pressure below the fracture pressure of formation in aim to dissolve matrix and make flow channels) and acid fracturing (injecting acid into the matrix pore structure with pressure above the fracture pressure of formation, leading to create fractures as well as channels). All these techniques can be used in all formations- carbonates or sandstones. But, the technique selected will depend on what the operation wishes to accomplish with the treatment (Bradley, 1987). Hydrochloric (HCl), Acetic (CH3COOH) and Formic (HCOOH) are the common acids are used to stimulate carbonate formations. Also Hydrofluoric (HF) acid is mainly acid to stimulate sandstone formations. In most of all sandstone cases, HF is not used alone, but it is used as a mixture with HCl, named as mud acid, in which HF may dissolve silicates as major components of matrix, where HCl may dissolve carbonate components and also depositions of drilling fluid on the wall of wellbore. In matrix acidizing, the process involves mainly three major stages: pre-flush, main flush and post-flush. The purpose of the pre-flush is to remove organic or inorganic scale from the wellbore tubulars prior to injection of acid. Aromatic solvent, such as xylene, can be used to remove hydrocarbon deposits. To remove rust and other inorganic scale, circulating 3-5% HCl downhole is adequate. The purpose of the main acid stage is to remove or bypass formation damages. The main acid stage is usually 15-28% HCl in carbonate formations. The purpose of the post-flush or over-flush stage is to displace acid to the perforations. Fresh water is the most common over-flush fluid. Filtered crude oil and diesel may also be used in oil wells, but are not preferred because of possible incompatibilities with acid. Nitrogen gas is an effective over-flush, especially in gas wells (Kalfayan, 2008). Many factors govern the reaction rate of an acid, such as: pressure, temperature, flow velocity and acid concentration. Reaction rate increases with acid concentration up to near 25% HCl, but not proportionally. Above 25%, the reaction rate decreases as a result of reduced acid concentration and the retarding effect of dissolved reaction products, such as calcium or magnesium chloride. Concentration may vary between 3% (for tubing cleaning application) and 35%. Acid solutions containing greater than 15% HCl are called high-strength acids. The most common field solution for matrix acidizing is 15% and 28% HCl, which is experimental optimum concentration in usual cases and in very tight carbonates respectively. (Mumallah, 1991). Many auxiliary chemicals have been developed to modify acid solution, such as corrosion inhibitors, Surfactants, silicate controlling agents, Iron controlling agents, gelling agents and fluid loss controlling agents (Mcleod, 1984).

Diverting agents are used for two purposes: 1- to divert acid in farther area in dense formations and create longer and more uniform channels. 2- In multi-layered reservoirs, to divert acid into sublayer with lower permeability- which is modelled in this paper. One of these materials which its application among well completion engineers and service companies is growing is gelled-acid containing visco-elastic surfactants (VESs). In 1958, White not only classified diverting agents into two major groups, but also had explained the chemical and physical considerations for using each agent, effect of several factors on their performance and factors affecting the choice of a blocking agent, such as type of formation, type of completion, pressure and temperature. The two major groups introduced by White were: 1- Materials which block by bridging at or near the well bore and affect an impermeable seal, such as: naphthalene, walnut-shell resin mixture, ammonium-chloride pellets and fines in thickened kerosene, and rock salts. 2- Materials which are pumped relatively far back into formation as a fluid and develop a gel structure to plug off the permeability, such as: heavy-metal soap-kerosene gel (White, 1958). Smith, et al. were the first team who used foams as diverting agents not (Smith, et al. 1969). This novel technique was followed by other researchers, leaded to other kinds of foam such as CO2 foam

and researches on its properties until now (Farajzadeh, et al. 2009), but because of limitations of this technique, such as pressure, temperature and permeability contrast, several researches have been done on other techniques of diversion, especially on gel diverters (Mehri Ghahfarrokhi, et al. 2019).

In a great discrepancy with foams, gelled acids are studied widely and used commercially in field operations scale. From first attempts until now, using these agents has a remarkable timeline with principal cornerstones, which are: first study of commercially available and high temperature stable polymers to generate gel (Norman, et al. 1984), use of in-situ cross-linked acids, i.e. ICAs, as the first generation of gelled acids and their performance in bottom hole injection (MaGee, et al. 1997), use of visco-elastic surfactant technology, VESs, in purpose to eliminate disadvantages of ICAs and reach better performance of gel (Gomaa, et al. 2011), successfully use of VES for diverting acid in a well (Chang, et al. 2001), investigation of the effect of factors affecting performance of gelled acid, such as cross-linker type and presence of corrosion inhibitors (Naser-El-Din, et al. 2006), salinity and HCl concentration (Miniawi, et al. 2007), initial permeability contrast (Ahmed, et al. 2008), and shear rate (Gomaa, et al. 2010) , stabilization of VES packages in high salinity brines such as high density completion brines (Van Zanten, 2011), finding the best concentration of VES to cause the highest viscosity (Al-Sadat, et al 2014), brilliant field success in using a self-diverting acid system based on a VES (Carpenter, 2014), finding harmful interactions between VES and Fe(III) on gelation (Shu, et al 2015), classification of recent technical advances in VESs in addition to their inherent limitations such as cost, applicable temperature range, and leak-off characteristics were reported (Hull, et al 2015). This timeline is completely reviewed in our previous paper (Mehri Ghahfarrokhi, et al. 2019).

Similar to other industrial operations, it is desirable to simulate gel-acid injection to predict how this operation is useful and which the best injection program is. Ratnakar et al. developed an empirical rheological model to describe the variation of the viscosity of in situ cross-linked acids with temperature, shear rate and pH. They presented a two-scale continuum model to describe reactive dissolution of carbonates with in-situ cross-linked acids and used it to analyze wormhole formation in single and dual core setups. They also compared wormhole formation with in-situ cross-linked acids to that with Newtonian acids, which are all acid solutions except gelled and foam acids in which viscosity of solutions have non-Newtonian behavior and is not constant, and showed that the in-situ crosslinked acids led to lower optimum injection rates and more branched wormholes as compared to Newtonian acids. They solved the two-scale continuum model, using operator splitting and implicit finite volume discretization where discretized equations were solved by advanced multigrid techniques to analyze the stimulation of single and dual core laboratory experiments with ICA for the case of constant injection rate (Ratnakar, et al. 2013).

In this study, a mathematical model is generated to simulate gel-acid injection process in one of Iranian Southwest oilfields (Ahwaz oilfield), and experimental data is compared with data predicted by the model.

2. Model description

We created a model consists of three equations and used it for simulating the gel-acid injection process into 2 core plug samples. Accurate solution of the model was obtained by using multigrid technique. This model is mostly similar to the model described by Maheshwari et al. for simple acidizing (Maheshwari, et al. 2013), but the difference is that in our model, viscosity is not constant and changes as a function of temperature and pH. Also, the model described by them was used for injection in one core (layer), but our model is used for simultaneous injection into two cores (layers) in which the flow distribution between these two cores is based on their instant permeability ratio. In this chapter, we introduce the model in details.

In this model, we use 3 equations to specify the flow behavior of injection fluid. These equations are:

1. Poisson's equation for the flow.
2. Convection-diffusion-reaction equation for balancing acid.
3. Viscosity-temperature-pH equation for representing viscosity as a function of temperature and pH.

To describe the flow, Poisson's equation, which is the combination of the Darcy's law and continuity equation, is used. Poisson's equation for the pressure field is given by:

$$\frac{\partial \phi}{\partial t} = -\nabla U = \nabla.(\frac{1}{\mu} K.\nabla P) \tag{1}$$

Where ∅ is the porosity, it is time, U = (U, V, W) is the Darcy velocity vector, K is the permeability tensor, P is the pressure and μ is the viscosity of the acid solution.

To specify balance for the acid, convection-diffusion-reaction equation is used. For linear kinetics, this equation is written as:

$$\frac{\partial \pi}{\partial t} + \nabla.(UC_f) = \nabla.(\phi D'_e.\nabla C_f) \tag{2}$$

$$\pi = \phi(C_f + \frac{\rho_s}{\alpha}) \tag{3}$$

Where C_f is the cup-mixing concentration of the acid in the fluid phase, D'_e is the effective dispersion tensor, ρ_s is the density of rock and α is the dissolving power of the acid, defined as grams of solid dissolved per mole of acid reacted.

As the dissolution proceeds, the local porosity is increased and is described in terms of the local acid cup-mixing concentration (C_f) by:

$$\frac{\partial \phi}{\partial t} = \frac{a_v \alpha}{\rho_s}(\frac{1}{k_s} + \frac{1}{k_c})^{-1} C_f = \frac{k_s k_c a_v \alpha}{(k_s + k_c)\rho_s} C_f \tag{4}$$

Where k_s is the dissolution rate constant; k_c is the local mass transfer coefficient and a_V is the interfacial area available for reaction per unit volume of the rock.

The initial and boundary conditions are given as follows:

$$UC_f - \phi D'_{eX} \frac{\partial C_f}{\partial x} = U_0 C_0 \text{ at x=0} \tag{5}$$

$$-\frac{K_x}{\mu}\frac{\partial P}{\partial x} = U_0, \frac{\partial P}{\partial y} = 0, \frac{\partial P}{\partial z} = 0 \text{ at x=0} \tag{6}$$

$$P = P_e, \frac{\partial C_f}{\partial x} = 0 \text{ at x=L} \tag{7}$$

$$n.\nabla P = 0, n.\nabla C_f = 0 \text{ on transverse boundaries} \tag{8}$$

$$\phi(l) = \phi_0 + \hat{f}, C_f = 0 \text{ at t=0} \tag{9}$$

where U is the axial component of velocity; U_0 is the axial component of injection velocity; D'_{eX} is the axial dispersion coefficient, C_0 is the inlet concentration of the acid; K_x is the axial permeability; P_e is the pressure at the exit boundary of the domain; L is the length of the core in the flow direction (x); n is the normal vector perpendicular to the transvers boundary; $\emptyset_0$ is the average initial porosity and $\hat{f}$ is random fluctuation in porosity. By means of random fluctuation ($\hat{f}$) in porosity, we introduce heterogeneity into the system which is needed to create unstable dissolution front leading to wormhole formation. This random number ($\hat{f}$) is assumed to be uniformly distributed in the interval [$-\Delta\emptyset_0$, $\Delta\emptyset_0$] and is added to the mean value of porosity $\emptyset_0$. The dimensionless length scale of heterogeneity (l) is defined as $l=l_{HT}/(2r_0)$, where l_{HT} is the heterogeneity length scale and r_0 is initial mean pore radius.

As dissolution proceeds, the structure of the porous medium changes continuously and so the local porosity, permeability and interfacial surface area also evolves with time. During dissolution, the fluid-solid interface changes in a complex manner, and in general, the relationship between these local quantities depends on the history of the dissolution process. Here, we use a modified Carman-Kozeny correlation to describe the increase in local permeability with local porosity due to dissolution that is given as follows:

$$K = KI \ , \ \frac{K}{K_0} = \frac{\phi}{\phi_0}\left(\frac{\phi(1-\phi_0)}{\phi_0(1-\phi)}\right)^{2\beta'} \tag{10}$$

Where K is the magnitude of local permeability; I is the identity tensor; K_0 is the initial average value of permeability and β' is pore broadening parameter.

The relative change in the mean pore radius (r_p) and the solid-fluid interfacial surface area (a_V) with respect to porosity is given by:

$$\frac{r_p}{r_0} = \sqrt{\frac{K\phi_0}{K_0\phi}} \ , \ \frac{a_V}{a_0} = \frac{\phi r_0}{\phi_0 r_p} \tag{11}$$

Where a_0 is the initial interfacial surface area per unit volume available for surface reaction.

Similarly, the mass-transfer coefficient and the effective dispersion coefficients are expressed using the correlations as follows:

$$Sh = \frac{2k_c r_p}{D_m} = Sh_\infty + 0.7\,\mathrm{Re}_p^{1/2} Sc^{1/3} \tag{12}$$

$$D'_{eX} = \alpha_{0s} D_m + \frac{2\lambda_X |U| r_p}{\phi} \ , \ D'_{eT} = \alpha_{0s} D_m + \frac{2\lambda_T |U| r_p}{\phi} \ \text{for T=y,z} \tag{13}$$

where Sh is the Sherwood Number or dimensionless mass transfer coefficient; Sh_∞ is the asymptotic Sherwood Number; Re_p is the pore scale Reynolds number defined as $Re_p = 2|U| r_p / v$; v is the kinematic viscosity; D_m is effective molecular diffusivity of acid; Sc is the Schmidt number defined as $Sc = v/D_m$; α_{0s} is a constant that depends on the pore connectivity; D'_{eX} is the longitudinal dispersion coefficient; D_{eT} is the transverse dispersion coefficient in y and z direction; λ_x and λ_T are constants which depend on the pore structure ($\lambda_x \approx 0.5$, $\lambda_T \approx 0.1$ for a packed-bed of spheres). The first term in mass transfer and dispersion correlations is molecular diffusion contribution that is dominant for small

pores or very low pore Reynolds numbers, while the second term is the convective contribution that is dominant for large pores or at higher Reynolds numbers.

Using the dimensionless variables below, the model can be re-written in dimensionless form. For simplicity of calculation, we consider a rectangular parallelepiped shaped core and define these parameters:

$$x' = \frac{x}{L},\ y' = \frac{y}{L},\ z' = \frac{z}{L},\ \alpha_y = \alpha_z = \frac{H'}{L},\ u = \frac{U}{U_0},\ t' = \frac{t}{(L/U_0)} \tag{14}$$

$$r = \frac{r_p}{r_0},\ A_V = \frac{a_V}{a_0},\ \kappa = \frac{K}{K_0},\ c_f = \frac{C_f}{C_0},\ p = \frac{P - P_e}{\frac{\mu U_0 L}{K_0}},\ \pi' = \frac{\pi}{C_0} \tag{15}$$

$$Da = \frac{k_s a_0 L}{U_0},\ \phi^2 = \frac{2k_s r_0}{D_m},\ \Phi^2 = \frac{k_s a_0 L^2}{D_m},\ N_{ac} = \frac{\alpha C_0}{\rho_s},\ \eta' = \frac{2r_0}{L} \tag{16}$$

where H' is the height/width of the domain; α_y and α_z are the aspect ratios in the transverse directions y and z, respectively; Dais Darnkohler number, defined as the ratio of convective time to reaction time based on the length of the core; $Ø^2$ is the pore-scale Thiele modulus, defined as the ratio of diffusion time to reaction time based on the initial pore size; Φ^2 is the macro-scale Thiele modulus which is the equivalent of the micro-scale Thiele modulus except it is defined at the core scale; N_{ac} is the acid capacity number, defined as the volume of solid dissolved per unit volume of the acid and η' is the ratio of two length scales: pore scale and core scale.

The non-dimensionless form of the equations and the initial and boundary conditions can be written as:

$$\frac{\partial \phi}{\partial t'} = -\nabla u = \nabla.(\frac{1}{\mu}\kappa.\nabla p) \tag{17}$$

$$\frac{\partial \pi'}{\partial t'} + \nabla.(uc_f) = \nabla.(\phi D_e.\nabla c_f) \tag{18}$$

$$\frac{\partial \phi}{\partial t'} = \frac{DaN_{ac}A_V c_f}{(1 + \frac{\phi^2 r}{Sh})} \tag{19}$$

$$\kappa = \kappa I\ ,\ \kappa = \frac{\phi}{\phi_0}(\frac{\phi(1-\phi_0)}{\phi_0(1-\phi)})^{2\beta'},\ r = \sqrt{\frac{\kappa\phi_0}{\phi}}\ ,\ A_V = \frac{\phi}{\phi_0 r} \tag{20}$$

$$D_{eX} = \frac{\alpha_{0s}Da}{\Phi^2} + \frac{\lambda_x |u| r\eta}{\phi}\ ,\ D_{eT} = \frac{\alpha_{0s}Da}{\Phi^2} + \frac{\lambda_T |u| r\eta}{\phi} \text{ for T=y,z} \tag{21}$$

$$c_f - \phi D_{eX}\frac{\partial c_f}{\partial x'} = 1 \text{ at x'=0} \tag{22}$$

$$-\frac{\kappa_x}{\mu}\frac{\partial p}{\partial x'} = u = 1,\ \frac{\partial p}{\partial y'} = 0,\ \frac{\partial p}{\partial z'} = 0 \text{ at x'=0} \tag{23}$$

$$p = 0,\ \frac{\partial c_f}{\partial x'} = 0 \text{ at x'=1} \tag{24}$$

$$n.\nabla p = 0,\ n.\nabla c_f = 0 \text{ on transverse boundaries} \tag{25}$$

$$\phi = \phi_0 + \hat{f} \ , \ c_f = 0 \ \text{at t'=0} \tag{26}$$

Where D_e is the effective dimensionless dispersion tensor; D_{ex} and D_{eT} are effective dimensionless axial/transverse dispersion coefficients, respectively; κ_x is the dimensionless axial permeability.

The model equations 17-21 along with the initial and boundary conditions in equations 22-26 are numerically solved. In each step, permeability of cores is re-calculated and flow distribution is pointed out. Also, concentration of acid in fluid is calculated and using equations below, viscosity of fluid is calculated.

To account the effect temperature on viscosity, a well-known equation is used expressed in term of the temperature coefficients of viscosity β as:

$$\mu = \mu_{0,T} \exp[-\beta \frac{T - T_0}{T_0}] \approx \mu_{0,T}[1 - \beta \frac{T - T_0}{T_0}] \tag{27}$$

Once applying 2 particular temperatures as T and T_0, with known viscosity of fluid at these 2 temperatures, the temperature coefficients of viscosity β can be calculated and applied for other temperatures.

As it was mentioned before in literature review, the gel-acid solutions based on VESs have a viscosity versus pH behavior in which viscosity remains constant in a lower limit value until pH reaches to a particular value (called pH of gelation), then viscosity increases gradually until an upper limit value and remains constant again. Figure 1 shows an example of viscosity versus pH behavior for a hypothetical solution containing VES.

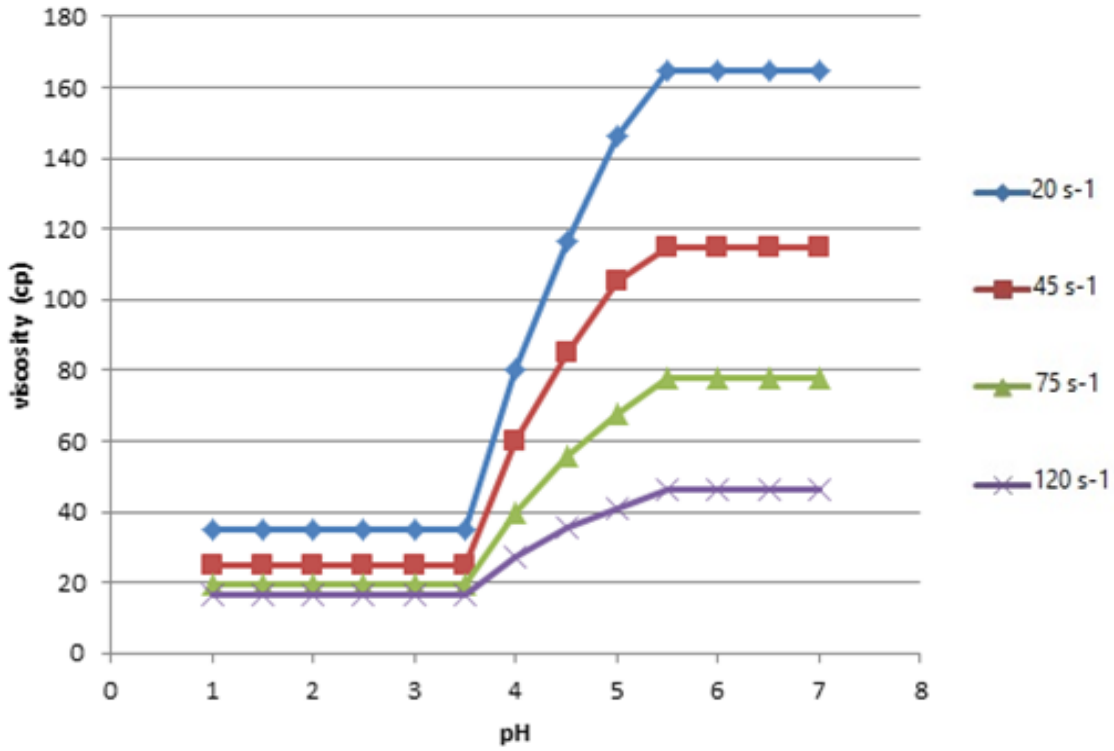

Figure 1

Viscosity versus pH in different shear rates for hypothetical solution containing VES.

The best mathematical fit for this behavior is sigmoidal. A sigmoid function is a mathematical function having an "S" shaped curve (sigmoid curve). A sigmoid function is a bounded differentiable real function that is defined for all real input values and has a positive derivative at each point. There are different types of sigmoid functions defined for curve-fitting software that can use them and generate a sigmoidal model for a sigmoid curve, for example:

- Gompertz Relation, y=a*exp(-exp(b-cx))
- Logisitic Model, y=a/(1+exp(b-cx))
- Richards Model, y=a/(1+exp(b-cx))^(1/d)
- Morgan-Morgan-Finney (MMF) Model, y=(ab+cx^d)/(b+x^d)
- Weibull Model, y=a-b*exp(-cx^d)

Each of above models has its limitations and accuracy. Working with a curve-fitting software revealed for us that the Morgan-Morgan-Finney (MMF) model has the best fit with our data. Figure 2 shows an example of curve fitting with MMF model.

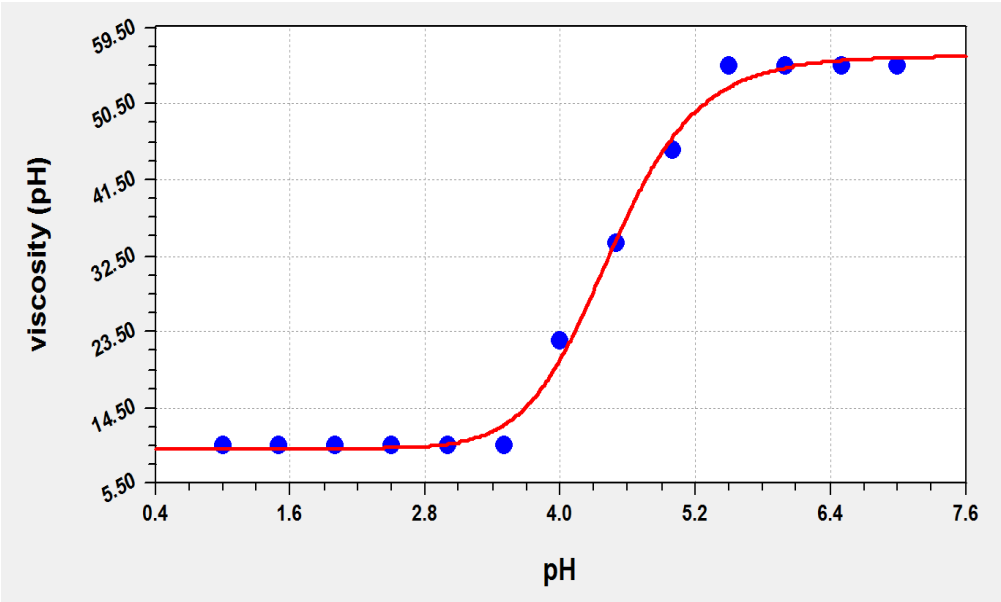

Figure 2

An example of curve fitting with MMF model (viscosity versus pH at shear rate=20s-1).

MMF model, as it was mentioned, is in the form:

$$y = \frac{ab + cx^d}{b + x^d} \tag{28}$$

Where a, b, c and d are constants. These constants must be calculated by curve-fitting for each case. For fitting this model to data gathered of a viscosity-pH test of a gel-acid solution, at first we must know which curve (which shear rate) must be used. This is because of different constant parameters (a, b, c and d) appear in case of each shear rate and any unique linear combination of shear rate and the parameters was found. So, normalizing parameter was impossible. Actually, even if normalizing was possible, it had not any benefits, because we can only use one particular shear rate for each material. So, it is better that curve-fitting be carried out for that particular shear rate. That particular shear rate, which is shear rate exerted to solution in porous media, is irrelevant to injection rate and is available in manufacturer company catalog for regular rock samples. It is obvious that if plugs are very highly compacted, highly loose or highly fractured, the shear rate that is reported by the company cannot be

used and must be calculated by porous media fluid flow equations. Curve-fitting for that particular shear rate with MMF model leads to equation:

$$\mu_0 = \frac{ab + cpH^d}{b + pH^d} \tag{29}$$

By combining equation 27 and equation 29, the viscosity-temperature-pH equation is obtained:

$$\mu = \frac{ab + cpH^d}{b + pH^d}[1 - \beta\frac{T - T_0}{T_0}] \tag{30}$$

In each step, viscosity is calculated by using equation 30. For solving differential equations, a code was generated in Matlab software, in which in all steps firstly viscosity is calculated then other equations are numerically solved. Any numerical divergences were occurred .

3. Results and discussion

Some parameters and dimensionless parameters must be fed into simulator to get predicted results of model. Table 1 shows these parameters. In addition to parameters mentioned above, parameters of the viscosity-temperature-pH equation must be known and fed to simulator. The viscosity-temperature-pH equation is in form equation 30.

As it was mentioned before, the temperature coefficient (β) for this fluid is calculated as a value of about 0.0285. By applying this value for β and T=100 and T0=25, the equation 30 will be:

$$\mu = 0.9\frac{ab + cpH^d}{b + pH^d} \tag{31}$$

Based on manufacturer company catalog for VES, shear rate exerted to fluid is 170 s-1. Figure 3 shows the curve-fitting for this shear rate by MMF model. The four parameters of MMF model are also listed in table 1.

Table 1

List of parameters used in simulation.

Dimensionless parameter	Value
Sh_∞	3
$\emptyset_{0\ low}$	0.13
$\emptyset_{0\ high}$	0.23
$\Delta\emptyset_0$	±0.15
α_{0s}	0.5
N_{ac}	0.05
B’	1
λ_x	0.5
λ_T	0.1
L	10 cm
r_0	1 μm
a_0	50 cm^{-1}

$K_{0\ high}$	6.14 md
$K_{0\ low}$	0.91 md
k_s	$1.4*10^{-4}$ cm/s
Dm	$4*10^{-6}$ cm^2/s
ρ_s	2.71 gr/cm^3
Initial fluid density	1.03 gr/cm^3
Vinj	0.044 cm/s
C_0	3.27 mol/lit
a	9.66083821465
b	$2.74571989776*10^7$
c	56.1088424503
d	11.4872873018

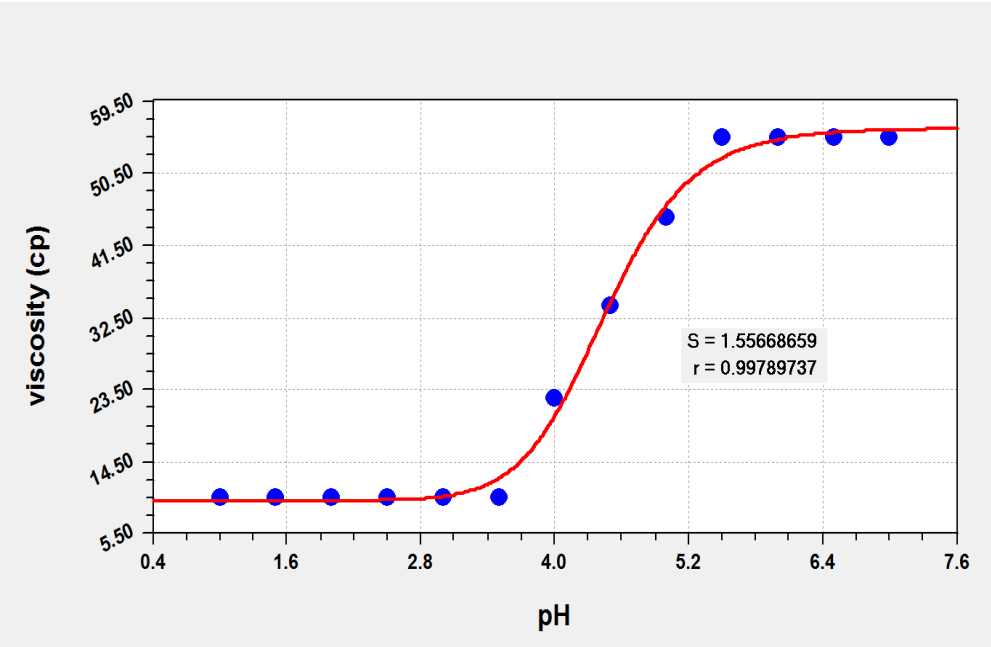

Figure 3

Curve-fitting by MMF model of viscosity versus pH of gelled-acid in the fourth set of injection test for shear rate= 170 s-1 at room temperature.

Table 2 contains the results generated by model and comparison between them and experimental data.

The above mentioned experimental data is from author's previous work. During that work, two kind of different visco-elastic surfactants (VES) provided by two different companies were used to produce gel to divert acid into a core plug sample having lower permeability in a dual acid injection set-up. The core plug samples were taken from pay zone of Ahwaz oilfield, one of Iranian Southwest oilfields. Before performing injection test, some viscosity measurement tests were carried out. Unfortunately, one of these two VESs had not an acceptable quality and injection tests by it were failed. But the other one passed all tests successfully and diverted the injection fluid.

.As it is obvious in table 2, the model can simulate the diversion phenomenon and permeability of cores (layers) after injection process with about 85% accuracy. The difference between experimental data and data generated by model can have several resources. At first, due to experimental records used, because HPHT viscometer was not available, the effect of pressure on gel formation and its viscosity was ignored. In addition to this, in modeling we have some assumptions which are maybe incorrect. For example, incomplete reaction due to remained CO2 produced by reaction of acid and rock and surfactant filtration due to difference in size of surfactant molecules and micropores in carbonate are neglected. Also, we used Carman-Kozeny correlation to describe the increase in local permeability with local porosity which is well suited for packed-beds, not for porous media in general.

Table 2

Experimental data and predicted data by model.

Core plug number	$K_{w\ before\ injection}$ (md)	$K_{w\ after\ injection}$ (md) by experiment	$K_{w\ after\ injection}$ (md) predicted by model	Difference (md-%)
7	6.14	18.5	16.2	2.3md-13%
8	0.91	12.5	14.3	2.2md-16%

٤. Conclusions and recommendations

The model which we developed can simulate the diversion phenomenon with an acceptable accuracy with experimental data (about 85%). This accuracy is high enough to use this model in industrial scale for modeling the injection process in oil wells. Also, some other studies could be done in aim to reach better accuracy. Sensitivity analysis by model for effect of injection rate, effect of permeability ratio and periodic injection of acid and gel-acid solution should be studied. If accurate experimental data for effect of injection rate, effect of permeability ratio and periodic injection of acid and gel-acid solution is available, the model can be tuned correctly and be used for designing injection program for each well and oilfield. In addition, the model should be revised to eliminate the assumptions that are presumed for simplification, but became sources of error for the model. Amongst them, complete reaction and removing CO2 is most important. To be more specific, instead of general Carman-Kozeny correlation to describe the relation between porosity and permeability, if results of R-CAL experiments on core plugs exist, once can use other correlations which are more suited for carbonate porous media.

Acknowledgement

I would like to appreciate Mr. Hamed Malhani and Mr. Seyed Mohsen Hosseini (well completion and stimulation, department of production, National Iranian South Oil Company) for their constant technical support and useful cooperation during this study.

Nomenclature:

a	: first matching parameter of MMF model
a_o	: initial interfacial area per unit volume available for surface reaction
a_v	: interfacial area per unit volume available for surface reaction
A_V	: dimensionless interfacial area per unit volume available for reaction
b	: second matching parameter of MMF model
c	: third matching parameter of MMF model
c_b	: dimensionless cup mixing concentration of the acid for the base case

c_f	: dimensionless cup mixing concentration of the acid
C_f	: cup mixing concentration of the acid
C_0	: inlet concentration of the acid
d	: fourth matching parameter of MMF model
D'_e	: effective dispersion tensor of the acid
D'_{eX}	: axial dispersion coefficient
D'_{eT}	: dispersion coefficient in transverse directions
D_{eX}	: dimensionless longitudinal dispersion coefficient
D_{eT}	: dimensionless dispersion coefficient in transverse directions
Da	: Darnkohler number
Da_{eff}	: effective Damkohler number
$\hat{f}$	: random fluctuation in porosity
H'	: height/width of the domain
I	: identity tensor
K	: permeability tensor
K_x	: permeability in axial direction
K_0	: initial average permeability of rock
k_c	: mass-transfer coefficient
k_s	: surface dissolution rate constant
k_{eff}	: effective volumetric reaction rate constant
l	: dimensionless heterogeneity length scale
l_{HT}	: heterogeneity length scale
L	: length of the core
N_{ac}	: acid capacity number
P	: dimensionless pressure
P	: pressure
P_e	: pressure at the exit boundary of the core
Pe_{eff}	: effective Peclet number
PV_{BT}	: pore volumes required to breakthrough
Q	: acid volumetric flow rate
Q_{opt}	: optimum acid injection rate
r	: dimensionless mean pore radius
r_p	: mean pore radius
r_0	: initial mean pore radius
Re_p	: pore scale Reynolds number
Sc	: Schmidt number
Sh	: Sherwood number
Sh_∞	: asymptotic value of Sherwood number
t	: time
t'	: dimensionless time
T	: temperature
u	: dimensionless velocity in axial direction
u_b	: dimensionless velocity in axial direction for the base case
U	: velocity in axial direction

U_0	: axial component of injection velocity
V	: transverse component of velocity in y direction
V_{inj}	: injection velocity
W	: transverse component of velocity in z direction
x	: axial/flow direction
x'	: dimensionless axial/flow direction
y,z	: transverse directions
y',z'	: dimensionless transverse directions
α	: dissolving power of acid
α_y	: aspect ratio in y direction
α_z	: aspect ratio in z direction
β	: temperature coefficients of viscosity
β'	: pore broadening parameter
γ	: shear rate
$\emptyset$	: porosity of the rock
$\emptyset_b$	: porosity of the rock for the base case
$\emptyset_0$	: initial mean porosity
$\Delta\emptyset_0$	: magnitude of heterogeneity
$\emptyset^2$	: pore-scale Thiele modulus
Φ^2	: macro-scale Thiele modulus
Φ'^2	: effective macro-scale Thiele modulus
H	: non-Newtonian viscosity
η'	: ratio of mean pore diameter to core length
κ	: dimensionless permeability tensor
κ_x	: dimensionless permeability in axial direction
μ	: viscosity
ρ_s	: solid density

References

Ahmed, W. A. F., Nasr-El-Din, H. A., Moawad, T. M. and Elgibaly, A., Effects of Crosslinker Type and Additives on The Performance on In-Situ Gelled Acids, SPE International Symposium and Exhibition on Formation Damage Control, Society of Petroleum Engineers, 2008.

Al-Sadat, W., Nasser, M., Chang, F., Nasr-El-Din, H., and Hussein, I., Rheology of A Viscoelastic Zwitterionic Surfactant Used in Acid Stimulation: Effects of Surfactant and Electrolyte Concentration, Journal of Petroleum Science and Engineering, Vol.124, p. 341-349, 2014.

Bradley, H. B., Petroleum Engineering Handbook, Society of Petroleum Engineers, USA, 1987.

Carpenter, C., 2014. Self-Diverting Acid for Effective Carbonate Stimulation Offshore Brazil, Journal of Petroleum Technology, Vol.66, No.06, p. 92-95.

Chang, F., Qu, Q. and Frenier, W., A Novel Self-diverting-acid Developed for Matrix Stimulation of Carbonate Reservoirs, SPE International Symposium on Oilfield Chemistry, Society of Petroleum Engineers, 2001.

Farajzadeh, R., Andrianov, A., Bruining, J. and Zitha, P. L. J., New Insights into Application of Foam for Acid Diversion. 8th European Formation Damage Conference, Society of Petroleum Engineers, 2009.

Gomaa, A. M. And Nasr-El-Din, H. A., New Insights into The Viscosity of Polymer-based in-situ-Gelled Acids, SPE Production & Operations, Vol.25, No. 03, p. 367-375, 2010.

Gomaa, A. M., and Nasr-El-Din, H. A., Propagation of Regular Hcl Acids in Carbonate Rocks: The Impact of an In Situ Gelled Acid Stage, Journal of Energy Resources Technology, Vol.133, No.2, p. 023101, 2011.

Hull, K. L., Sayed, M., and Al-Muntasheri, G. A., Recent Advances in Viscoelastic Surfactants for Improved Production from Hydrocarbon Reservoirs, SPE International Symposium on Oilfield Chemistry, Society of Petroleum Engineers, 2015.

Kalfayan, L., Production Enhancement with Acid Stimulation, Pennwell Books, South Sheridan Road, Tulsa, Oklahoma, USA, 2008.

Magee, J., Buijse, M. and Pongratz, R., Method for Effective Fluid Diversion when Performing A Matrix Acid Stimulation in Carbonate Formations, Middle East Oil Show and Conference, Society of Petroleum Engineers, 1997.

Mcleod, H. O., Matrix Acidizing, Journal of Petroleum Technology, Vol.36, No.12, p. 2,055-2,069. 1984.

Mehri Ghahfarrokhi, A., Kazemzadeh, E., Shokrollahzadeh Behbahani, H., Safian, Gh. A., An Experimental Study of Acid Diversion by Using Visco-elastic Surfactants based Gelled Acid Systems: Case Study in One of Iranian Southwest Oilfields, Iranian Journal of Oil and Gas Science and Technology, Vol.8, No. 1, p. 32-46, 2019.

Miniawi, M. A., Ahmed, W. A. F., Ali, Y., and Soufi, A. R., In Situ Gelled Acid as A Diverting System in Water Injection Well, SPE/IADC Middle East Drilling and Technology Conference, Society of Petroleum Engineers, 2007.

Mumallah, N., Factors Influencing the Reaction Rate of Hydrochloric Acid and Carbonate Rock, SPE International Symposium on Oilfield Chemistry, Society of Petroleum Engineers, 1991.

Nasr-El-Din, H. A., Chesson, J. B., Cawiezel, K. E., and De Vine, C. S., Field Success in Carbonate Acid Diversion, Utilizing Laboratory Data Generated by Parallel Flow Testing, SPE Annual Technical Conference and Exhibition, Society of Petroleum Engineers, 2006.

Norman, L. R., Conway, M. W., and Wilson, J. M., Temperature-stable Acid-gelling Polymers: Laboratory Evaluation and Field Results, Journal of Petroleum Technology, Vol.36, No. 11, p. 2, p.011-2,018,1984.

Shu, Y., Wang, G., Nasr-El-Din, H. A., and Zhou, J., Interactions of Fe (III) and Viscoelastic-surfactant-based Acids, SPE Production & Operations, 2015.

Smith, C. L., Anderson, J. L. and Roberts, P., New Diverting Techniques for Acidizing and Fracturing, SPE California Regional Meeting, Society of Petroleum Engineers, 1969.

Van Zanten, R., Stabilizing Viscoelastic Surfactants in High-density Brines, SPE Drilling & Completion, Vol.26, No.04, p. 499-505, 2011.

White, G., The Use of Temporary Blocking Agents in Fracturing and Acidizing Operations, Drilling and Production Practice, American Petroleum Institute, 1958.